Physics Letters A 375 (2011) 2327–2332

Contents lists available at ScienceDirect

Physics Letters A

www.elsevier.com/locate/pla

Stability of traveling pulses of cubic–quintic complex Ginzburg–Landau equation including intrapulse Raman scattering

M. Facão [a,*], M.I. Carvalho [b]

[a] Department of Physics, I3N, University of Aveiro, Campus Universitário de Santiago, 3810-193 Aveiro, Portugal
[b] DEEC/FEUP and INESCPorto, University of Porto, Rua Dr. Roberto Frias, 4200-465 Porto, Portugal

ARTICLE INFO

Article history:
Received 20 January 2011
Received in revised form 9 April 2011
Accepted 12 April 2011
Available online 4 May 2011
Communicated by A.P. Fordy

ABSTRACT

The complex cubic–quintic Ginzburg–Landau equation (CGLE) admits a special type of solutions called eruption solitons. Recently, the eruptions were shown to diminish or even disappear if a term of intrapulse Raman scattering (IRS) is added, in which case, self-similar traveling pulses exist. We perform a linear stability analysis of these pulses that shows that the unstable double eigenvalues of the erupting solutions split up under the effect of IRS and, following a different trajectory, they move on to the stable half-plane. The eigenfunctions characteristics explain some eruptions features. Nevertheless, for some CGLE parameters, the IRS cannot cancel the eruptions, since pulses do not propagate for the required IRS strength.

1. Introduction

The complex cubic–quintic Ginzburg–Landau equation (CGLE) models several physical systems which are at the emergence of spatio-temporal patterns. Examples in the optical context are pulse propagation in fibers with linear and nonlinear gain and spectral filtering [1–4] or pulse generation in fiber lasers with additive pulse mode-locking or nonlinear polarization rotation [5,6]. Among the large variety of solutions admitted by this equation, we find solitary solutions that propagate without change of form, giving them the status of solitons [7–13]. Since the model is non-conservative, the CGLE solitons belong to the group of so-called dissipative solitons, and their stationary propagation results from the balance of dispersion and nonlinearity but also of gain and loss.

Here, we have particular interest on a special kind of CGLE solitons named *erupting* solitons. As their name anticipates, they propagate as a stationary single pulse for a while, until they develop side perturbations that grow and achieve amplitudes that surpass the amplitude of the single pulse itself, then these perturbations break up and split in small humped waves which fade away. The single pulse survives to this eruption and propagates steadily for another distance. The process repeats indefinitely with a period that is not exactly constant. The erupting solitons have been found numerically [12] on a relatively large region of the CGLE parameter space, and were experimentally observed in passively mode-locked lasers [14]. Recently, the eruptions were shown to change or even cancel by the introduction of one or more additional terms in the CGLE [15–18]. In fact, in [18] we have shown that the intrapulse Raman scattering (IRS), if sufficiently strong, may stabilize the propagation of the single pulse on the eruption parameter region, thus eliminating the eruptions. Below this threshold of IRS strength, the eruptions pattern is also different which may be noticed on, for instance, the frequency and symmetry of the eruption. The observed steady pulses are slightly asymmetric and travel with a velocity that is larger than the group velocity of the initial central frequency. Actually, they are traveling self-similar solutions of the CGLE plus IRS that exist for the whole parameter region of eruptions as shown in [18]. Here we investigate the linear stability spectrum of these self-similar solutions using a Evans function method in order to understand the change of behavior and eventual cancellation of eruptions caused by the IRS.

The evolution equation under study and their traveling solutions are presented in Section 2. The linear stability problem, its main characteristics and the results of the Evans function method are in Section 3. In Section 4, we present the results of full numerical simulations of the evolution equation and compare them with the stability results. Finally we conclude in Section 5.

* Corresponding author.
E-mail addresses: mfacao@ua.pt (M. Facão), mines@fe.up.pt (M.I. Carvalho).

0375-9601/$ – see front matter
doi:10.1016/j.physleta.2011.04.051

2. Traveling solutions

Let us first introduce the evolution equation that consists on the CGLE in the anomalous-dispersion regime plus a term that represents the IRS, namely

$$iq_Z + \frac{1}{2}q_{TT} + |q|^2 q = i\delta q + i\beta q_{TT} + i\epsilon|q|^2 q + i\mu|q|^4 q - \nu|q|^4 q + T_r\left(|q|^2\right)_T q \tag{1}$$

where, in the optical context, q is the normalized envelope of the optical field and Z and T are the normalized propagation distance and retarded time, respectively. The parameters in this equation are all normalized versions of the actual parameters, namely, δ stands for linear gain/loss, ϵ for nonlinear gain, $\mu<0$ for the saturation of nonlinear gain, $\nu<0$ for the saturation of the Kerr effect and T_r for the intrapulse Raman scattering.

Here, we are interested in a range of CGLE parameters for which erupting solitons have been found (see Fig. 5 of [12]), that is a region on the parameter plane (ν,ϵ) for fixed $\beta=0.125$, $\delta=-0.1$ and $\mu=-0.1$. Recently [18], we have shown that, on the above region, Eq. (1) admits traveling single-hump solutions. These solutions are of the form $q(Z,T)=F(\tau)e^{i\theta(\tau)+i\omega Z}$ (F and θ real), with $\tau=T-\upsilon Z$. Inserting this *ansatz* into (1), we obtain

$$\left(\frac{1}{2}+2\beta^2\right)F'' + 2\left(\beta\upsilon - T_R F^2\right)F' + (2\beta\delta-\omega)F + \upsilon\frac{M}{F} - \left(\frac{1}{2}+2\beta^2\right)\frac{M^2}{F^3} + (1+2\beta\epsilon)F^3 + (\nu+2\beta\mu)F^5 = 0, \tag{2}$$

$$\left(\frac{1}{2}+2\beta^2\right)M' + 2\beta\upsilon M - \left(\upsilon+4\beta T_R F^2\right)FF' - (2\beta\omega+\delta)F^2 + (2\beta-\epsilon)F^4 + (2\beta\nu-\mu)F^6 = 0 \tag{3}$$

where $M=F^2\theta'$. The integration of those ordinary differential equations showed that the profiles of amplitude F and phase θ, as well as the values of ω, are almost identical to the ones corresponding to $T_r=0$. The major difference of the solution as T_r varies is the velocity υ, that is proportional to T_r and is negative. Hence, and before we proceed to obtain the linear stability equations for those solutions, let us first make some considerations about the velocity υ. For this purpose, let us note that numerical simulations and results from a perturbation approach have shown that the nonlinear Schrödinger equation plus small effects of linear loss, spectral filtering and IRS (i.e., CGLE with $\epsilon=\nu=0$) exhibits equilibrium pulse solutions close in shape to the NLS solitons, but that travel with fixed positive velocity that is proportional to T_r [19]. This also implies that the solutions mean frequency down-shifts, which is an effect consistent with the Stokes Raman response that the IRS term is modeling. However, the CGLE plus IRS has equilibrium pulse solutions that travel with negative velocity or, equivalently, they have a frequency shift to higher values. The explanation for this frequency shift may be associated with the non-conservative nature of the CGLE that permits amplification of any spectrum side of the initial input.

It is also interesting to verify that the sign of υ is associated with the shape of the stationary beams amplitude. In effect, if we assume that, at the tails, $F(\tau)=F_0 e^{g\tau}$ and $M(\tau)=N_0 e^{2g\tau}$, introduce them in (2) and (3) and neglect terms higher than $\exp(g\tau)$ in (2) and higher than $\exp(2g\tau)$ in (3), we obtain

$$\left(\frac{1}{2}+2\beta^2\right)g^2 - 2\beta\upsilon g - \left(\frac{1}{2}+2\beta^2\right)\alpha^2 + \upsilon\alpha + 2\beta\delta - \omega = 0$$

where

$$\alpha = \frac{\upsilon g+\delta+2\beta\omega}{g+4\beta^2 g+2\beta\upsilon}.$$

Then, following the Ferrari procedure to solve quartic equations [20], we obtain two complex conjugate solutions and two real solutions given by

$$g_{1,2} = \pm\sqrt{y_+} - \frac{2\beta\upsilon}{1+4\beta^2}$$

where y_+ is real and positive. Since $\upsilon<0$, this result implies that the decay rate at the right, which corresponds to the negative g, should be smaller in absolute value than the positive g associated with the left tail. Thus, the traveling pulses are asymmetric, having a longer right tail with a slower decay rate. Note that exactly the opposite type of asymmetry is found in the stationary solutions of the nonlinear Schrödinger equation plus IRS [21].

3. Linear stability equations

Since numerical simulations show that for each set of the CGLE parameters there is a threshold of the strength of IRS that we must reach in order to observe stable propagation of the traveling pulses discussed above, we proceed to investigate this effect by studying their linear stability spectrum. For this purpose, let us consider the above traveling solution plus a small perturbation term $q(Z,T)=[F(\tau)e^{i\theta(\tau)}+\Delta(Z,\tau)]e^{i\omega Z}$. Demanding that Δ has exponential dependence on Z, i.e., $\Delta(Z,\tau)=u(\tau)e^{i\lambda Z}+x^*(\tau)e^{-i\lambda^* Z}$ we obtain the following stability eigenvalue problem

$$L\mathbf{w}=\lambda\mathbf{w}, \quad \mathbf{w}=(u \quad x)^T \tag{4}$$

where

$$L=\begin{pmatrix} (\frac{1}{2}-i\beta)\partial_{\tau\tau} - i\upsilon\partial_\tau - \omega - i\delta + 2(1-i\epsilon)F^2 \\ \quad -3(i\mu-\nu)F^4 - T_r(3FF' + F^2\partial_\tau - i\theta' F^2) & [(1-i\epsilon)F^2 - 2(i\mu-\nu)F^4 \\ & \quad - T_r(FF' + F^2\partial_\tau + i\theta' F^2)]e^{2i\theta} \\ [-(1+i\epsilon)F^2 + 2(-i\mu-\nu)F^4 & -(\frac{1}{2}+i\beta)\partial_{\tau\tau} - i\upsilon\partial_\tau + \omega - i\delta - 2(1+i\epsilon)F^2 \\ \quad + T_r(FF' + F^2\partial_\tau - i\theta' F^2)]e^{-2i\theta} & \quad + 3(-i\mu-\nu)F^4 + T_r(3FF' + F^2\partial_\tau + i\theta' F^2) \end{pmatrix}.$$

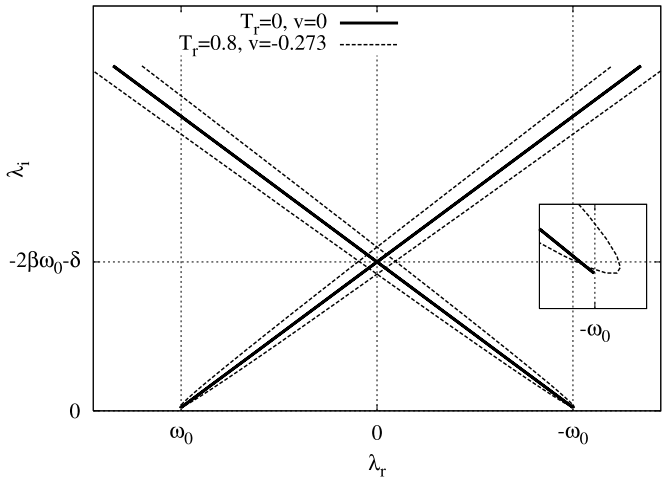

Fig. 1. Continuous spectrum for $\delta = -0.1$, $\beta = 0.125$, $\mu = -0.1$, $\epsilon = 1.0$, $\nu = -0.6$ and $T_r = 0$ and 0.8. The inset shows the details of the line starting point and the parabola vertex.

The traveling pulses are linearly stable if L has no eigenvalues λ with negative imaginary part. Due to the symmetry of (4) relatively to the imaginary axis, we expect that whenever there is an eigenvalue λ with associated eigenfunction $(u\ x)^T$, there also exists an eigenvalue $-\lambda^*$, corresponding to the eigenfunction $(x^*\ u^*)^T$. Therefore, in the following, only the eigenvalues with positive real part will be considered. Moreover, the spectrum of L consists of a continuous set and discrete eigenvalues. One trivial discrete eigenvalue is $\lambda = 0$, which corresponds to the translational and rotational invariances of the PDE (1). Thus, in this case, this zero eigenvalue is double and the modes are easily recognized as $(Fe^{i\theta}\ -Fe^{-i\theta})^T$ and $((F' + i\theta' F)e^{i\theta}\ (F' - i\theta' F)e^{-i\theta})^T$. The other discrete eigenvalues will be evaluated below using the Evans function method. The location of the continuous spectrum may be estimated using the continuous spectrum of the limiting form of L for $\tau \to \pm\infty$ which reads

$$L_\infty = \begin{pmatrix} (\frac{1}{2} - i\beta)\partial_{\tau\tau} - i\upsilon\partial_\tau - \omega - i\delta & 0 \\ 0 & -(\frac{1}{2} + i\beta)\partial_{\tau\tau} - i\upsilon\partial_\tau + \omega - i\delta \end{pmatrix}.$$

The continuous spectrum of L_∞ is composed by two oblique parabolas on the λ-plane defined by $(1/2 - i\beta)s^2 - \upsilon s + \omega + i\delta + \lambda = 0$ and $(1/2 + i\beta)s^2 + \upsilon s + \omega - i\delta - \lambda = 0$, with s being any real number. Let us first consider $T_r = 0$, in which case the parabolas are degenerate since $\upsilon = 0$. In this latter case, the continuous spectrum consists of two lines starting at $(\omega_0, -\delta)$ or $(-\omega_0, -\delta)$ (where ω_0 stands for ω at $T_r = 0$) and extending to the upper half-plane with slope -2β and 2β, respectively. Whenever $T_r \neq 0$, υ is also nonzero and we obtain two properly parabolas that are also in the upper half-plane for $\delta < 0$. The axes of symmetry of these parabolas have slopes equal to the lines that constitute the continuous spectrum for $T_r = 0$ and their vertex are at $(\omega - (0.5 + 4\beta^2)\upsilon^2/(1 + 4\beta^2)^2, -\delta + \beta\upsilon^2/(1 + 4\beta^2)^2)$ and $(-\omega + (0.5 + 4\beta^2)\upsilon^2/(1 + 4\beta^2)^2, -\delta + \beta\upsilon^2/(1 + 4\beta^2)^2)$ which, for the considered β and calculated ω's and υ's, are very close to the starting points of the above lines. Note that the lowest point of these parabolas are $(\omega, -\delta)$ and $(-\omega, -\delta)$ which almost coincide with the starting points of the lines for $T_r = 0$ since the only difference is the tiny difference between ω_0 and the actual ω for each T_r (see Fig. 1). Following Henry [22], the continuous spectrum of L itself is on the regions defined by the lines that constitute the continuous spectrum of L_∞, so that, it is on or inside the above parabolas. Hence, the continuous stability spectrum of these solutions is stable if $\delta < 0$, which is consistent with the assumption that we need linear gain to be negative for linear waves to extinguish.

We searched for discrete eigenvalues, especially the ones with negative imaginary part, using the approach of Alexander et al. of the Evans function method [23,24]. Due to the analyticity of the Evans function away from the continuous spectrum, the existence of unstable eigenvalues was investigated by calculating the Evans function around a semicircle with large radius whose straight line stands on the real axis, and then applying the argument principle. In order to avoid the $\lambda = 0$ eigenvalue, we have deformed the semicircle close to the origin using another semicircle, this one with a very small radius. To confirm our results, we have also computed these eigenvalues by considering the discretized operator L, which was obtained by evaluating (4) in equidistant points and using finite-differences, and then applying sparse matrix methods.

The results for $T_r = 0$ are similar to the ones obtained in [25], i.e., we found a double eigenvalue at the origin and, in the right half-plane, one double unstable eigenvalue for higher values of ϵ and two double unstable eigenvalues for smaller values of ϵ. Even though three pairs of unstable discrete eigenvalues are referred in [25] for small ϵ, we did not find more than two pairs for the CGLE parameters considered here.

As we introduce T_r, the double eigenvalues split up and travel in the direction of the real axis. For a large part of the studied eruption parameter region, namely, the upper part of the strip (Fig. 5 of [12]), these eigenvalues reach the real axis hence they turn to stable discrete eigenvalues. However, for CGLE parameters in the lower part of the strip we are unable to observe the eigenvalue most unstable (larger imaginary absolute value) crossing the real axis, since for sufficiently large T_r we cannot find the pulse profiles using our shooting procedure. This difficulty suggests that for these CGLE parameters, the traveling solutions do not exist. Fig. 2(a) shows the trajectories on the lower half-plane of the discrete eigenvalues as T_r increases for two sets of CGLE parameters in the upper strip of the eruption region. As already mentioned, we have only represented the eigenvalues that have positive real part since the trajectory of their counterpart with negative real part is identical. Note that the double eigenvalue for $T_r = 0$ has real part identical to the correspondent ω_0, that is 17.26 for $\epsilon = 1.0$ and 41.42 for $\epsilon = 1.5$. We have also noted that as we change ϵ or ν, the real part of these eigenvalues are following the corresponding $\pm\omega_0$ that are the real parts of the tips of the continuous spectrum.

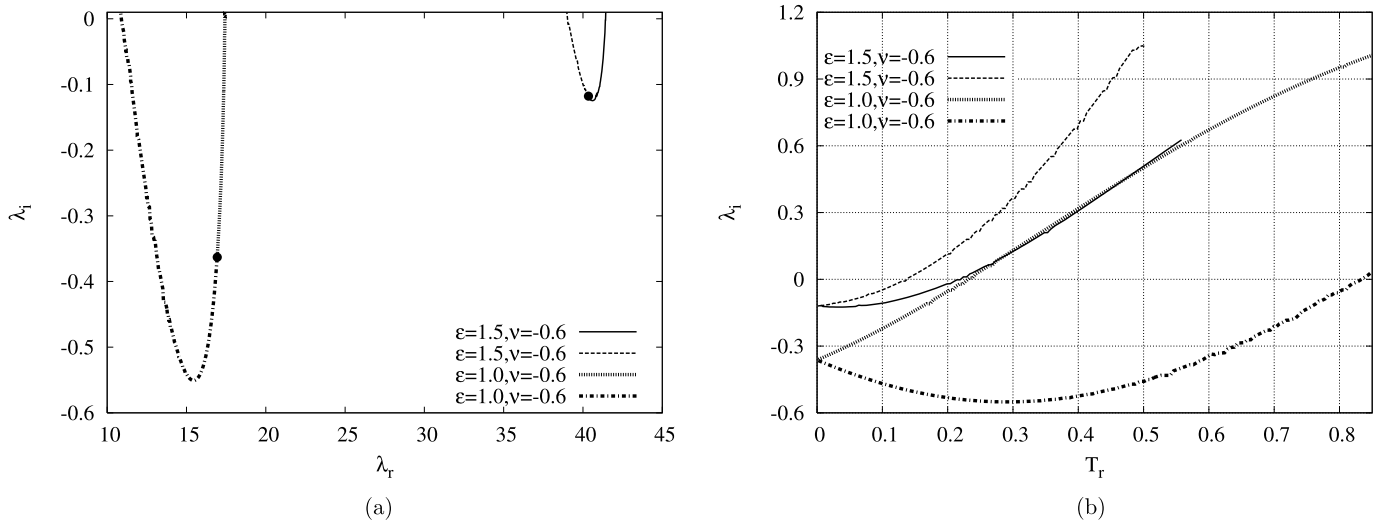

Fig. 2. (a) Trajectories of unstable eigenvalues as T_r varies for two sets of CGLE parameters, all having $\delta = -0.1$, $\beta = 0.125$, $\mu = -0.1$ and ϵ and ν as indicated in the labels. (b) Evolution of imaginary part of each discrete eigenvalue with T_r. The two branches for each set correspond to the different trajectories followed by each eigenvalue that splits from the double eigenvalue at $T_r = 0$.

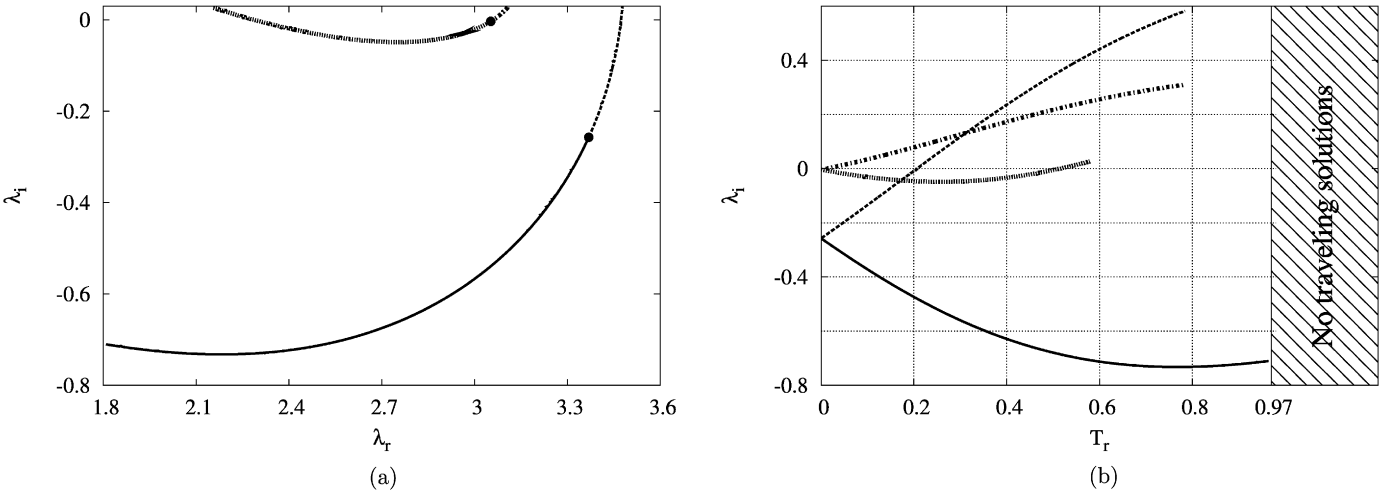

Fig. 3. (a) Trajectories of the two unstable eigenvalues as T_r varies for $\delta = -0.1$, $\beta = 0.125$, $\mu = -0.1$, $\epsilon = 0.5$ and $\nu = -0.6$. (b) Evolution of imaginary part of each discrete eigenvalue with T_r.

For a given CGLE parameter set in the eruption region, the crossing of the real axis occurs at distinct values of T_r for each eigenvalue. This can be seen in Fig. 2(b), which depicts the evolution of the imaginary part of each eigenvalue, using the same line code that was used in Fig. 2(a). For the $\epsilon = 1.0$, $\nu = -0.6$ case, we have found that the first discrete eigenvalue enters the stable region when $T_r = 0.24$, whereas the second one only becomes stable for $T_r > 0.84$. For the other case represented ($\epsilon = 1.5$ and $\nu = -0.6$), these threshold values of T_r are 0.14 and 0.22. Note that, at $T_r = 0$, the unstable double eigenvalue for $\epsilon = 1.0$ is deeper in the unstable region than it is for $\epsilon = 1.5$, which may explain the higher threshold values of T_r that occur for $\epsilon = 1.0$. Also note that in the first case it is the eigenvalue that has the largest λ_r that first becomes stable, while the opposite happens in the second case.

In Fig. 3, we represent the trajectory of the four unstable eigenvalues that are situated at the right half-plane for $\epsilon = 0.5$ and $\nu = -0.6$ (lower strip of the eruption region). Three of the eigenvalues reach the stable region for reasonably low T_r values. The last of these enters the stable region at $T_r = 0.52$. The fourth eigenvalue is still deeper in the unstable region at $T_r = 0.95$ and, for these CGLE parameters, we are unable to find profiles above this value of T_r. Similar results were obtained for other values of (ϵ, ν) on the lower strip of the eruption region that is here studied.

Using the discretized operator L we have also computed the eigenfunctions associated with each unstable eigenvalue. Fig. 4 shows these functions for the case $\epsilon = 1.0$, $\nu = -0.6$ and $T_r = 0.2$. Due to the symmetry of L, only the eigenfunctions corresponding to the eigenvalues with positive real part are represented. Note that both u and x are located to the right of the solitary beam for the eigenvalue with the largest real part, whereas the opposite can be observed for the other eigenvalue. The same result was obtained in every case we studied, and it leads to interesting conclusions. In effect, three different propagation scenarios are expected. When the T_r value is not enough to turn stable any discrete eigenvalue, we expect that explosions occur periodically at both sides of the erupting soliton but exhibiting an asymmetry with a preferred side. Let us refer that asymmetric explosions were already reported for the CGLE without any other higher order term [26,27], but in this case they are occurring on both sides along the soliton propagation and they do not appear in any preferred side. As T_r increases such that one eigenvalue pair crosses the real axis, explosions should only occur at the side where the eigenfunctions of the still unstable eigenvalue pair are located. Note that in this case the system shows a pure asymmetric explosion,

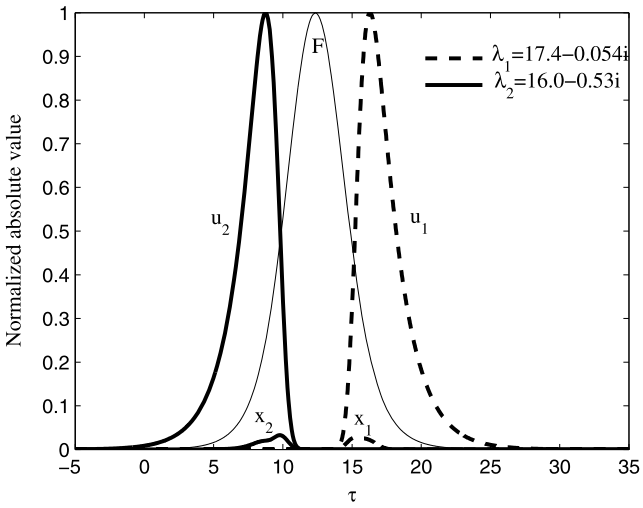

Fig. 4. Eigenfunctions corresponding to the unstable discrete eigenvalues with positive real part for the previous values of δ, β and μ, and for $\epsilon = 1.0$, $\nu = -0.6$ and $T_r = 0.2$.

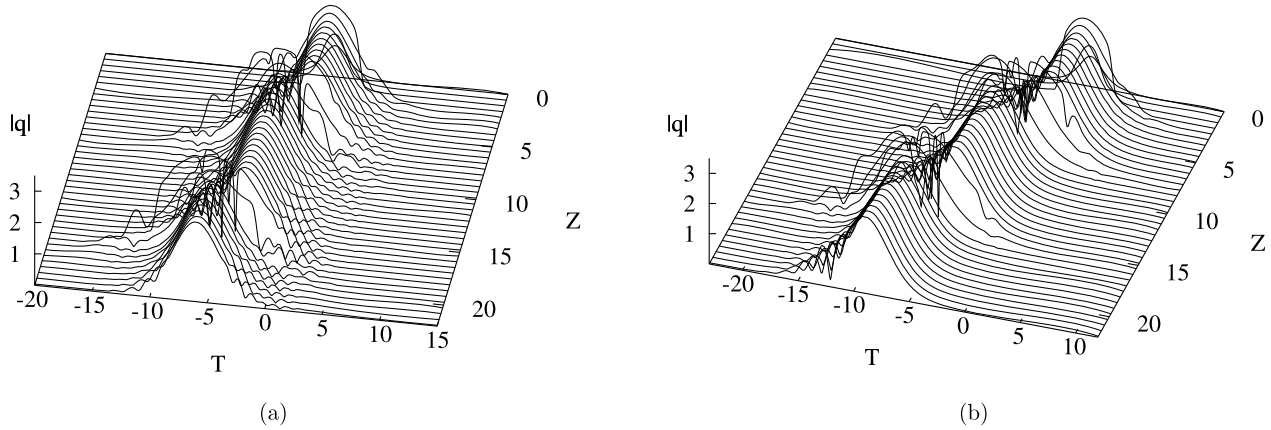

Fig. 5. Profile evolution under Eq. (1) for $\delta = -0.1$, $\beta = 0.125$, $\mu = -0.1$, $\epsilon = 1.0$, $\nu = -0.6$ and (a) $T_r = 0.15$ and (b) $T_r = 0.3$.

only left or right depending on the unstable eigenfunction, so the explosive behavior is distinct from the one observed for the CGLE only. Finally, when the value of T_r is high enough to make all the discrete eigenvalues enter the stable region, explosions should be completely eliminated.

4. Full numerical simulation

The three different beam evolutions predicted by the stability analysis in the above section can be easily observed by PDE numerical simulations. In order to better excite any existing unstable mode, the *sech* profile was used as input in all our simulations. As a first example, we let $\epsilon = 1.0$ and $\nu = -0.6$, and consider both $T_r = 0.15$ and $T_r = 0.3$, which correspond, respectively, to two and one discrete unstable eigenvalues with positive real part. As expected, the propagation for the first case, represented in Fig. 5(a), exhibits intermittent explosions on both sides of the beam but reasonable asymmetric due to the different growth rate associated with the left and right eigenmodes. The asymmetry picks always the same side of the soliton, even for longer distances. In the second case, however, the explosions are only observed on the left side of the beam (see Fig. 5(b)), and this is also the case for long propagation distances. Effectively, as Fig. 2 indicates, for this set of (ϵ, ν) parameters, the first eigenvalue to become stable is the one with the largest real part, for which the eigenfunctions are located to the right of the beam. Thus, in this case, it is expected that the explosions on the right side of the beam are eliminated by IRS, which is consistent with the results presented in Fig. 5(b). Also according to Fig. 2, exactly the opposite behavior should be observed for $\epsilon = 1.5$ and $\nu = -0.6$, and for a T_r value between the first and the second threshold values, since in this case the eigenfunctions of the still unstable eigenvalue, the one with the largest real part, are located to the right of the stationary beam. The explosions on this side of the beam can be clearly observed in Fig. 6(a), which depicts the evolution for $\epsilon = 1.5$, $\nu = -0.6$, and for $T_r = 0.18$. Finally, Fig. 6(b) shows the stable propagation of the stationary beam for the previous (ϵ, ν) values and $T_r = 0.3$, for which all discrete eigenvalues are already stable.

We have also simulated the propagation for CGLE parameters corresponding to the lower strip of the erupting region and for different values of T_r. We have found that propagation in this region is only possible for relatively small values of T_r. The worst case we obtained occurred for $\epsilon = 0.35$ and $\nu = -0.8$, for which we observed the pulse fading out with Z for $T_r = 0.2$ This implies that traveling solutions do not exist in this lower strip for higher values of T_r, and explains the already mentioned difficulties with the shooting method in this region. Also note that, unlike what happens in this lower strip, this pulse fading out only occurs, in the upper strip, for relatively higher T_r values, such as $T_r = 2.0$ for $\epsilon = 1.2$ and $\nu = -1.06$.

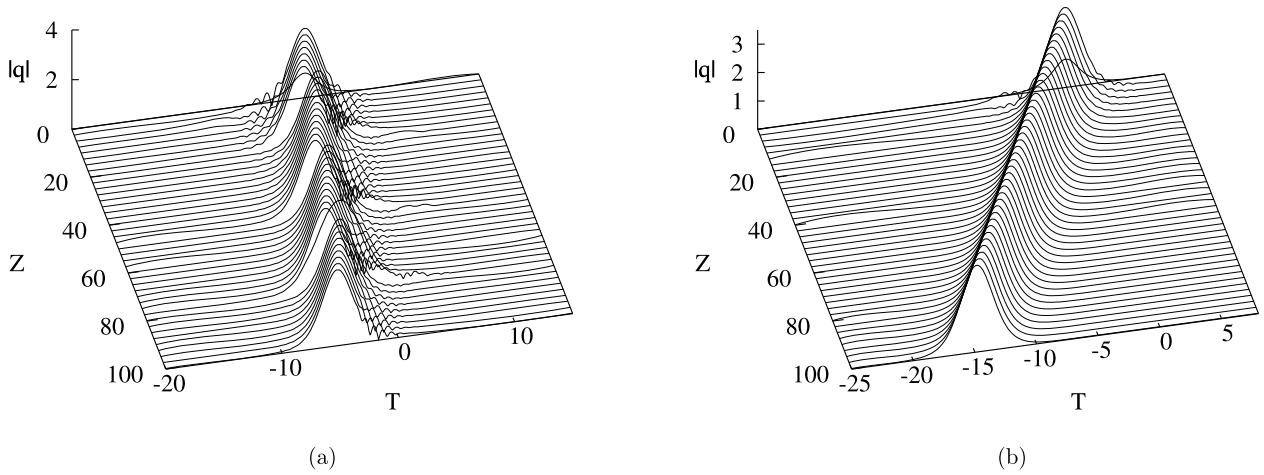

Fig. 6. Profile evolution under Eq. (1) for $\delta = -0.1$, $\beta = 0.125$, $\mu = -0.1$, $\epsilon = 1.5$, $\nu = -0.6$ and (a) $T_r = 0.18$ and (b) $T_r = 0.3$.

5. Conclusions

We have performed a stability analysis of the previously found traveling pulses for the CGLE plus IRS. The continuous spectrum, that consisted of two oblique lines in the absence of IRS, is in this case composed by two parabolas that are in the stable half-plane. The discrete double unstable eigenvalues, which are associated with the eruptions, split up in the presence of IRS and, in general, move in the direction of the stable half-plane, as was expected since the cancellation of the eruptions under the influence of IRS was already observed. For this cancellation to occur, it is known that a minimum strength of IRS must be used. This minimum of T_r, that depends on CGLE parameters, is anticipated by our stability results since it corresponds to the T_r value at which the last unstable eigenvalue enters the stable region. We have also searched for the eigenfunctions and found that to each eigenvalue that splits from the double eigenvalue at $T_r = 0$ is associated one eigenfunction that is only situated on the right or on the left-hand side of the pulse profile. Since the two eigenvalues do not enter the stable half-plane for the same T_r, this eigenfunction characteristic explains the asymmetric eruptions that were observed immediately below the T_r threshold for stable propagation. Moreover, we have also observed that, in the lower strip of the eruptions region (lower ϵ), the IRS cannot cancel the eruptions since the trajectory of one of the unstable eigenvalues enters deep into the unstable region, and the pulse propagation becomes impossible for relatively low values of T_r also in this region.

An interesting analysis would be about the physical reasons of the reduction or cancellation of eruptions with the introduction of the intrapulse Raman scattering. Some numerical experiences suggest that the perturbations that arise during the explosions have their spectra inside the spectrum of the main pulse where the spectral filtering is not very efficient and possibly the Raman scattering move them to the spectrum sides where the spectral filtering is more active. However, a full analysis is left for a following work.

References

[1] A. Mecozzi, J. Moores, H. Haus, Y. Lai, Opt. Lett. 16 (1991) 1841.
[2] Y. Kodama, A. Hasegawa, Opt. Lett. 17 (1992) 31.
[3] L.F. Mollenauer, J. Gordon, S. Evangelides, Opt. Lett. 17 (1992) 1575.
[4] M. Matsumoto, H. Ikeda, T. Uda, A. Hasegawa, J. Lightwave Technol. 13 (1995) 658.
[5] H.A. Haus, J.G. Fujimoto, E. Ippen, J. Opt. Soc. Am. B 8 (1991) 2068.
[6] J.D. Moores, Opt. Commun. 96 (1993) 65.
[7] N.N. Akhmediev, V.V. Afanasjev, Phys. Rev. Lett. 75 (1995) 2320.
[8] N.N. Akhmediev, V.V. Afanasjev, J.M. Soto-Crespo, Phys. Rev. E 53 (1996) 1190.
[9] V.V. Afanasjev, N. Akhmediev, J.M. Soto-Crespo, Phys. Rev. E 53 (1996) 1931.
[10] J.M. Soto-Crespo, N.N. Akhmediev, V.V. Afanasjev, S. Wabnitz, Phys. Rev. E 55 (1997) 4783.
[11] N. Akhmediev, A. Ankiewicz, J. Soto-Crespo, Phys. Rev. Lett. 79 (1997) 4047.
[12] J.M. Soto-Crespo, N. Akhmediev, A. Ankiewicz, Phys. Rev. Lett. 85 (2000) 2937.
[13] J.M. Soto-Crespo, N. Akhmediev, K.S. Chiang, Phys. Lett. A 291 (2001) 115.
[14] S.T. Cundiff, J.M. Soto-Crespo, N. Akhmediev, Phys. Rev. Lett. 88 (2002) 73903.
[15] H.P. Tian, Z.H. Li, J.P. Tian, G.S. Zhou, J. Zi, Appl. Phys. B 78 (2004) 199.
[16] L. Song, L. Li, Z. Li, G. Zhou, Opt. Commun. 249 (2005) 301.
[17] S.C.V. Latas, M.F.S. Ferreira, Opt. Lett. 35 (2010) 1771.
[18] M. Facão, M.I. Carvalho, S.C. Latas, M.F. Ferreira, Phys. Lett. A 374 (2010) 4844.
[19] K.J. Blow, N.J. Doran, D. Wood, J. Opt. Soc. Am. B 5 (1988) 1301.
[20] L.E. Dickson, Elementary Theory of Equations, Bibliolife, 2009.
[21] M. Facão, M. Carvalho, D. Parker, Phys. Rev. E 81 (2010) 046604.
[22] D. Henry, Geometric Theory of Semilinear Parabolic Equations, 3rd ed., Lecture Notes in Math., vol. 840, Springer-Verlag, Berlin, 1993.
[23] J. Alexander, R. Gardner, C. Jones, J. Reine Angew. Math. 410 (1990) 167.
[24] M. Facão, M.I. Carvalho, Proc. Nonlinear Phys.: Theory Exp. 160 (2009) 917.
[25] N. Akhmediev, J.M. Soto-Crespo, Phys. Lett. A 317 (2003) 287.
[26] N. Akhmediev, J.M. Soto-Crespo, Phys. Rev. E 70 (2004) 036613.
[27] O. Descalzi, H.R. Brand, Phys. Rev. E 82 (2010) 026203.